Nuclear Spin-Lattice Relaxation in Antiferromagnetic FeF_2

M. BUTLER* AND TIN NGWE*†
Department of Physics, University of California, Santa Barbara, California 93106

AND

N. KAPLAN*‡
Department of Physics, University of California, Santa Barabra, California 93106
and Physics Department, Hebrew University, Jerusalem, Israel

AND

H. J. GUGGENHEIM
Bell Telephone Laboratories, Murray Hill, New Jersey 07971

(Received 10 March 1969)

The nuclear spin-lattice relaxation (NSLR) of F^{19} nuclei in antiferromagnetic FeF_2 has been studied experimentally and theoretically, and is shown to be due to a two-magnon Raman scattering process. The assumption of isotropic magnon dispersion allows simplification of the calculations while still including zone-boundary effects. This model adequately describes the total density of states for generally cubic crystals whose exchange interaction may be expressed by a single parameter. However, processes which depend on magnon scattering, such as NSLR, can be calculated with reasonable accuracy only for relatively dispersionless spin-wave spectra. This is due to replacing the true cubic Brillouin zone, in which different directions in k space do not contribute equally to the density of states, with the model's spherical Brillouin zone in which all directions contribute equally. Comparison of the FeF_2 data with those for the isostructural antiferromagnet MnF_2 indicates that the temperature above which NSLR is insensitive to changes in anisotropy is much lower than the corresponding temperature for magnetization data.

INTRODUCTION

RECENTLY, Kaplan *et al.*[1] have shown that the longitudinal relaxation T_1 of F^{19} nuclei in antiferromagnetic MnF_2 is brought about by Raman scattering of thermally excited magnons via the anisotropic hyperfine interaction.[2] The isostructural antiferromagnet FeF_2 differs from MnF_2 primarily in that there is a sizable initial gap kT_{AE} in the magnon spectrum caused by the large crystalline anisotropy of the Fe^{2+} ion. We have studied the F^{19} T_1 in an attempt to understand the effect anisotropy plays in determining the relaxation rate.

The experiments were carried out on single crystals of zone-refined FeF_2 using standard spin-echo techniques. The recovery of the nuclear magnetization was exponential with a characteristic time T_1.

PHYSICAL PROPERTIES OF FeF_2 AND MnF_2

FeF_2, like MnF_2, is a uniaxial antiferromagnet with the rutile structure shown in Fig. 1. The magnetic ions form a body-centered tetragonal lattice with the spin moments of the corner and body-centered ions aligned antiparallel. This is due to J_2 being the dominant exchange. J_1 and J_3, which couple spins along the c and a axes, respectively, are quite small and may be neglected. The FeF_2 lattice parameters differ by less than 5% from those of MnF_2 as can be seen in Table I. Similarly, their Néel temperatures are reasonably close. The two difluorides differ primarily in their anisotropy constants.

The spin-wave dispersion relation for these two crystals may be written[3]

$$\epsilon(k)=2SZ_2|J_2|[(1+\xi)^2-\gamma^2(k)]^{1/2}, \qquad (1)$$

where

$$\gamma(k)=\cos(\tfrac{1}{2}ak_x)\cos(\tfrac{1}{2}ak_y)\cos(\tfrac{1}{2}ck_z),$$

$$\xi=\frac{H_A}{2SZ_2|J_2|}-\frac{2Z_1J_1}{Z_2J_2}\sin^2(\tfrac{1}{2}ck_z)-\frac{Z_3J_3}{Z_2J_2}[\sin^2(\tfrac{1}{2}ak_x)+\sin^2(\tfrac{1}{2}ak_y)],$$

S is the spin of the magnetic ion, the coordination

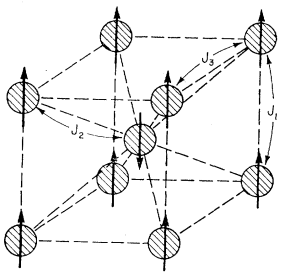

FIG. 1. Magnetic unit cell of FeF_2 showing the possible exchange parameters. Only the Fe^{2+} ions are shown.

* Supported in part by the National Science Foundation.
† Present address: Physics Department, University of California, Riverside, California.
‡ Present address: Physics Department, Hebrew University, Jerusalem, Israel.
[1] N. Kaplan, R. Loudon, V. Jaccarino, H. J. Guggenheim, D. Beeman, and P. A. Pincus, Phys. Rev. Letters **17**, 357 (1966).
[2] For a general review of NSLR in antiferromagnets see D. Beeman and P. A. Pincus, Phys. Rev. **166**, 359 (1968).
[3] A. Okazaki, K. C. Turberfield, and R. W. H. Stevenson, Phys. Letters **8**, 9 (1964).

numbers $Z_1=2$, $Z_2=8$, and $Z_3=4$, a and c are the magnetic unit-cell dimensions, the J's are appropriate exchange parameters, $\mathbf{k}$ is the spin-wave momentum, and H_A is the effective anisotropy field seen by each ion. From this, one sees that a large effective anisotropy field H_A will cause a large gap in the spin-wave spectrum at $k=0$. A comparison of representative dispersion curves for FeF_2[4] and MnF_2[3] is shown in Fig. 2.

One might expect the density of states in FeF_2 and MnF_2 to be quite different because of the disparity in the initial spin-wave gaps. This, however, is not the case. The density of states $D(E)$ is directly proportional to $\int d\mathbf{k}$, where the integral is over a volume in $\mathbf{k}$ space bounded by constant energy surfaces at E and $E+dE$. As this volume gets larger at higher energies, the largest density of states occurs at the zone boundary. Increasing the anisotropy increases the minimum spin-wave energy, which effectively pushes states to higher energies. However, since the number of states moved to a higher energy is small compared to the existing density of states at that energy, they have little effect. Thus, the larger anisotropy cuts off the low-energy tail of the spectrum and has relatively little effect on the peak in the density of states at the zone boundary.

TABLE I. Physical properties of FeF_2 and MnF_2.

	a (Å)	c (Å)	T_N (°K)	J_1 (°K)	J_2 (°K)	J_3 (°K)	H_A (°K)
FeF_2	4.70[a]	3.31[a]	78.12[b]	−0.03[c]	−2.60[c]	0.14[c]	27.7[c]
MnF_2	4.87[a]	3.31[a]	67.34[d]	0.32[e]	−1.76[e]	0.00[e]	1.06[e]

[a] Reference 6.
[b] G. K. Wertheim and D. N. Buchanan, Phys. Rev. **161**, 478 (1967).
[c] Reference 4.
[d] P. Heller, Phys. Rev. **146**, 403 (1966).
[e] Reference 3.

T_1 PROCESSES INVOLVED

Nuclear spin-lattice relaxation in antiferromagnetic insulators arises when a nuclear spin interacts with the spin-wave spectrum via the "hyperfine" interaction. Here in "hyperfine" we include all electron-nucleus interactions. Because of the large gap, the minimum allowed spin-wave energy is much larger than the nuclear Zeeman energy, and therefore the direct process in which a single magnon is emitted or absorbed is not allowed in FeF_2 or MnF_2 due to energy conservation. When expanding the components of the electronic spin in magnon operators, one finds only S_z contains a term corresponding to the destruction of one and the creation of a second magnon. To change the nuclear quantum number M_z by one unit, the interaction must couple to I_x or I_y. Thus a two-magnon process can only occur if off-diagonal elements exist in the hyperfine coupling tensor. This mechanism is allowed in both $FeF^{19}{}_2$ and $MnF^{19}{}_2$, and as has been shown[1] is the dominant process in MnF_2. The three-magnon process, which was considered for MnF_2 and was shown to be one order of magnitude less important,[1] is not allowed in FeF_2 because of energy conservation. In such a process one creates two and destroys one magnon, or vice versa, and therefore twice the minimum available spin-wave energy must be less than the maximum spin-wave energy: $2\omega_{\text{gap}}<\omega_{\max}$. This condition cannot be satisfied for FeF_2, since $\omega_{\text{gap}}=0.66\omega_{\max}$. Thus one is led to the conclusion that the fluorine nuclear spin-lattice relaxation in FeF_2 proceeds via two-magnon Raman scattering. Contributions to $1/T_1$ from the magnon-phonon coupling[5] have been considered and are found to be orders of magnitude too small.

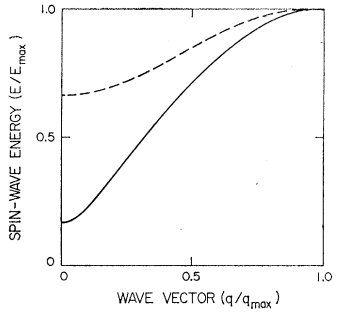

FIG. 2. Comparison of spin-wave dispersion. The solid line is MnF_2 and the dashed line FeF_2.

In FeF_2 each fluorine nucleus is coupled via the transferred hyperfine interaction to three neighboring Fe^{2+} spins as shown in Fig. 3. The off-diagonal terms in the hyperfine-interaction tensor come mainly from the dipolar fields of spins I and I'. This interaction may be written

$$\mathcal{H}'=I_yA_{yz}{}^IS_z{}^I+I_yA_{yz}{}^{I'}S_z{}^{I'}. \tag{2}$$

The symmetry of the crystal requires that $A_{yz}{}^I=-A_{yz}{}^{I'}$, so that the static hyperfine fields at the fluorine site arising from these terms cancel.[6] However, the dynamic relaxation of the fluorine nuclei by these terms does not vanish.

According to theory,[7–9] the longitudinal relaxation rate $1/T_1$ in an antiferromagnet has an angular dependence

$$\frac{1}{T_1}=\frac{1}{T_1{}^0}+\frac{1}{T_1{}'}\sin^2\theta, \tag{3}$$

where θ is the angle between the axes of quantization of the nuclear and electronic spins. In the antiferromagnet FeF_2, the Fe^{2+} electronic spins are collinear with the

[4] H. J. Guggenheim, M. T. Hutchings, and B. D. Rainford, J. Appl. Phys. **39**, 1120 (1968).

[5] P. Pincus and J. Winter, Phys. Rev. Letters, **7**, 269 (1962).
[6] A. M. Clogston, J. P. Gordon, V. Jaccarino, M. Peter, and L. R. Walker, Phys. Rev. **117**, 1222 (1960).
[7] T. Moriya, Progr. Theoret. Phys. (Kyoto) **16**, 23 (1956); **16**, 641 (1956).
[8] J. Van Kranendonk and M. Bloom, Physica **22**, 545 (1956).
[9] A. Mitchell, J. Chem. Phys. **27**, 59 (1957).

crystalline c axis. The resultant hyperfine field at each fluorine nucleus, arising from the three neighboring magnetic ions, points along the c axis (see Fig. 3). Thus $\theta=0$ in FeF_2 and zero-field measurements will give us $1/T_1^0$.

The angular-dependent part of Eq. (3) can be measured by applying a static field H_{app} perpendicular to the c axis (see Fig. 3). Under this condition the resultant field H_r at the F^{19} site is $(H_{hf}^2+H_{app}^2)^{1/2}$, and makes an angle $\theta=\tan^{-1}(H_{app}/H_{hf})$ with the c axis. The directions of the magnetic spins are essentially unchanged by H_{app} because it is small compared to the exchange field [i.e., the electron spins are canted by the angle $\varphi=\sin^{-1}(H_{app}/2H_{ex})$]. Thus by measuring $1/T_1$ as a function of H_{app} perpendicular to the c axis, one can determine $1/T_1'$.

It was shown[1] that the appropriate expressions for $1/T_1^0$ and $1/T_1'$ are

$$\left(\frac{1}{T_1^0}\right)_{\text{two-magnon}}=\frac{4\pi}{\hbar N^2}(A_{yz}{}^I)^2\sum_{\mathbf{k},\mathbf{k}'}(u_{\mathbf{k}}{}^2u_{\mathbf{k}'}{}^2+v_{\mathbf{k}}{}^2v_{\mathbf{k}'}{}^2)\frac{\exp(E_{\mathbf{k}}/k_BT)}{[\exp(E_{\mathbf{k}}/k_BT)-1]^2}\sin^2[(\mathbf{k}-\mathbf{k}')\cdot(\mathbf{r}^I-\mathbf{r}^{I'})/2]\delta(E_{\mathbf{k}}-E_{\mathbf{k}'}) \quad (4a)$$

and

$$\left(\frac{1}{T_1'}\right)_{\text{two-magnon}}=\frac{\pi}{\hbar N^2}\sum_{\mathbf{k},\mathbf{k}'}\{(2(A_{zz}{}^I)^2+(A_{zz}{}^{II})^2)(u_{\mathbf{k}}{}^2u_{\mathbf{k}'}{}^2+v_{\mathbf{k}}{}^2v_{\mathbf{k}'}{}^2)+2(A_{zz}{}^I)^2$$
$$\times(u_{\mathbf{k}}{}^2u_{\mathbf{k}'}{}^2+v_{\mathbf{k}}{}^2v_{\mathbf{k}'}{}^2)\cos((\mathbf{k}-\mathbf{k}')\cdot(\mathbf{r}^I-\mathbf{r}^{I'}))-4A_{zz}{}^IA_{zz}{}^{II}u_{\mathbf{k}}u_{\mathbf{k}'}v_{\mathbf{k}}v_{\mathbf{k}'}$$
$$\times[\cos((\mathbf{k}-\mathbf{k}')\cdot(\mathbf{r}^I-\mathbf{r}^{II}))+\cos((\mathbf{k}-\mathbf{k}')\cdot(\mathbf{r}^{I'}-\mathbf{r}^{II}))]\}\frac{\exp(E_{\mathbf{k}}/k_BT)}{[\exp(E_{\mathbf{k}}/k_BT)-1]^2}\delta(E_{\mathbf{k}}-E_{\mathbf{k}'}). \quad (4b)$$

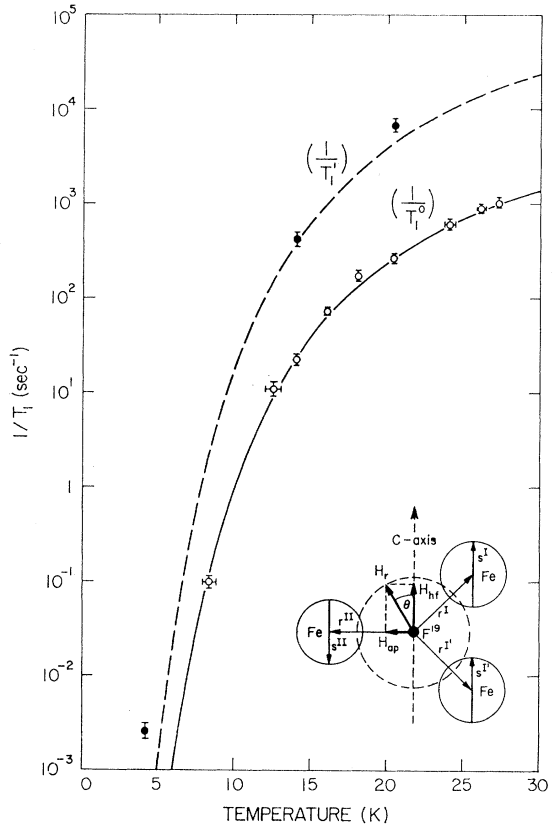

FIG. 3. Longitudinal relaxation of F^{19} in FeF_2. Solid and dashed curves are the rates calculated for $1/T_1^0$ two-magnon and $1/T_1'$ two-magnon, respectively. The insert shows the symmetry of the fluorine site.

In these expressions $E_{\mathbf{k}}$ is the energy of the magnon of wave vector $\mathbf{k}$, and the remaining notation is that of Ref. 10.

MODEL CALCULATION

Both T_1^0 and T_1' have been calculated numerically for F^{19} in MnF_2,[1] and the agreement between experiment and theory was found to be excellent in the temperature region of interest (i.e., where noninteracting spin-wave theory is applicable). We have instead calculated the same quantities for F^{19} in FeF_2 using a simplified model for evaluating Eqs. (4a) and (4b).

The model is useful only for generally cubic crystals whose magnetic properties are dominated by a single exchange interaction, a condition which is satisfied for FeF_2, where $|J_1/J_2|=0.01$ and $|J_3/J_4|=0.05$.[4] In this case for the rutile structure the spin-wave dispersion relation (1) becomes

$$E(q)=2SZ_2|J_2|[(1+\xi)^2-\gamma^2(q)]^{1/2}, \quad (5)$$

where

$$\xi=H_A/2SZ_2|J_2|, \quad \gamma(q)=\cos\tfrac{1}{2}q_x\cos\tfrac{1}{2}q_y\cos\tfrac{1}{2}q_z.$$

Here q is the reduced wave vector and related to $\mathbf{k}$ by $q_i=k_ix_i$, where x_i is the length of the unit cell in the i direction.

The approximation of our model consists of replacing $\gamma(q)$ by

$$\gamma(q)=\cos(\tfrac{1}{2}q). \quad (6)$$

[10] Review article by V. Jaccarino, in *Magnetism*, edited by G. T. Rado and H. Suhl (Academic Press Inc., New York, 1963), Vol. 2A, Chap. 5.

That is to say, we assume the spin-wave spectrum is isotropic in reduced space—the surfaces of constant energy in q space are spherical. This has the effect of redistributing the states of large q value. However, since the dispersion relation is relatively flat in this region, the energy of these states is changed very little. As a consequence the density-of-states function is essentially unaffected. The total number of states is conserved by normalization of the new density of states. Using this approximation, Eqs. (4a) and (4b) can be reduced to one-dimensional integrals on energy as is shown in the Appendix. Equation (4a) becomes

$$\frac{1}{T_1^0}=\frac{4\pi}{\hbar}(A_{yz}{}^I)^2\left(\frac{A}{2[2(A_{zz}{}^I)^2+(A_{zz}{}^{II})^2]}-\frac{B}{4(A_{zz}{}^I)^2}\right), \quad (7a)$$

and Eq. (4b) becomes

$$1/T_1'=(\pi/\hbar)(A+B-2C), \quad (7b)$$

where

$$A=[2(A_{zz}{}^I)^2+(A_{zz}{}^{II})^2]\int_{E_{\min}}^{E_{\max}} D^2(E)F(E)C(E)\frac{E_0}{E}dE,$$

$$B=\frac{48}{\pi^3(E_0)}(A_{zz}{}^I)^2\int_{E_{\min}}^{E_{\max}} D(E)C(E)F(E)$$
$$\times\left[(1+\xi)^2-\left(\frac{E}{E_0}\right)^2\right]^{1/2}\left\{\left[1+\left(\frac{E}{E_0}\right)^2\right]-(1+\xi)^2\right\}^{1/2}dE,$$

and

$$C=\frac{96}{\pi^3}A_{zz}{}^IA_{zz}{}^{II}(E_0)^2\int_{E_{\min}}^{E_{\max}} D(E)$$
$$\times\frac{(1+\xi)^2}{E^3}\left[(1+\xi)^2-\left(\frac{E}{E_0}\right)^2\right]^{1/2}$$
$$\times\left[1-\left(\frac{E}{E_0}\right)^2-(1+\xi)^2\right]^{1/2}F(E)dE,$$

where the notation is explained in the Appendix.

Figure 3 shows the comparison between theory and experiment. The zero-field relaxation rate calculated using expression (7a) for the F^{19} nuclei in FeF_2 was fitted to the experimental data by adjusting $A_{yz}{}^I$. The $A_{yz}{}^I$ value for a best fit to the experimental data is 7.1×10^{-4} cm^{-1}. This may be compared to an $A_{yz}{}^I$ value of 5.4×10^{-4} cm^{-1} used to fit the $MnF^{19}{}_2$ data.[1] The calculated $(T_1')^{-1}$ values contain no adjustable parameters as $A_{zz}{}^I$ and $A_{zz}{}^{II}$ were previously determined by Stout and Shulman.[11] The 4.2°K point for $1/T_1'$ is suspect, since it requires T_1 measurements on the order of several hours, thus making it very susceptible to "paramagnetic" impurity effects.

It is to be noted that the present approximation is a considerable improvement on the so-called long-wavelength approximation in that it does include zone-boundary effects in a reasonable way. Although this reproduces a reasonable total density of states, there are distortions introduced into k space by changing the Brillouin zone from cubic to spherical. At a given energy, different directions in a cubic Brillouin zone contribute differently to the density of states, while for a spherical one, all directions contribute equally. Thus the probability of a magnon scattering in a given direction in k space will be different for cubic and spherical Brillouin zones. This changes the average value of the sine-squared term in the relaxation rate equation (4a). These distortions are enhanced for a crystal having more than one exchange such as MnF_2. Here, due to a significant J_1, the zone-boundary magnon peak splits, corresponding to two directions in reciprocal space.[12] The inadequacy of the model, where all directions in **k** space contribute equally to the density of states, to account for this anisotropy in phase space is pointed up in Fig. 4. Here the exact zero-field two-magnon relaxation rate[1] for $MnF^{19}{}_2$ is compared to the model calculation using identical parameters. At higher temperatures, where the zone-boundary magnons dominate, the approximation overestimates the relaxation rate because the magnons have preferred scattering angles due to the anisotropy in phase space. These preferred scattering directions tend to preserve the z component of momentum, and thus reduce the angular factor in the relaxation rate equation (4a). At lower temperatures, where the anisotropy in the dominant part of the spin-wave spectrum is less, the error is still large because the function containing the angular factor is the difference

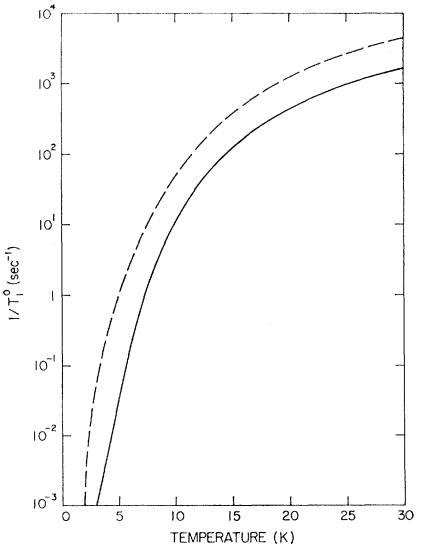

FIG. 4. Zero-field longitudinal relaxation of F^{19} in MnF_2. The solid curve is the exact calculation (Ref. 1) and the dashed curve is calculated using the present approximation.

[11] J. W. Stout and R. G. Shulman, Phys. Rev. **118**, 1136 (1960).

[12] S. J. Allen, R. Loudon, and P. L. Richards, Phys. Rev. Letters **16**, 463 (1966).

between two large quantities. Thus small errors in either term can produce significant errors in the relaxation rate. The present approximation has also been applied to susceptibility calculations[13] in MnF_2 with good results. This is because the susceptibility only depends on the total density of states and not their angular distribution in k space.

Thus we may summarize the conditions under which the present approximation is useful as follows:

(a) The magnetic ions must form a generally cubic lattice and the exchange must be describable by a single exchange parameter.

(b) For two-magnon or higher-order processes, the spin-wave spectrum must be relatively dispersionless (i.e., a large gap at $k=0$).

COMPARISON OF FeF_2 AND MnF_2 RESULTS

Judging by the range over which the relaxation rate may vary, it might appear surprising that the FeF^{19}_2 NSLR is so similar to the MnF^{19}_2 results. As can be seen in Fig. 5, the ratio R of these relaxation rates is flat above $\sim 0.1kT/E_{zB}$ and rises sharply below this temperature. The sharp rise is due to the relaxation rate no longer being dominated by the zone-boundary magnons; thus MnF_2 with a smaller gap tends to have a faster relaxation rate. The fact that the ratio is not unity above $0.1kT/E_{zB}$ may be partially explained by the difference in $A_{yz}{}^I$ values. A plot of the ratio

$$M=\frac{(\Delta m/m)(\mathrm{MnF_2})}{(\Delta m/m)(\mathrm{FeF_2})},$$

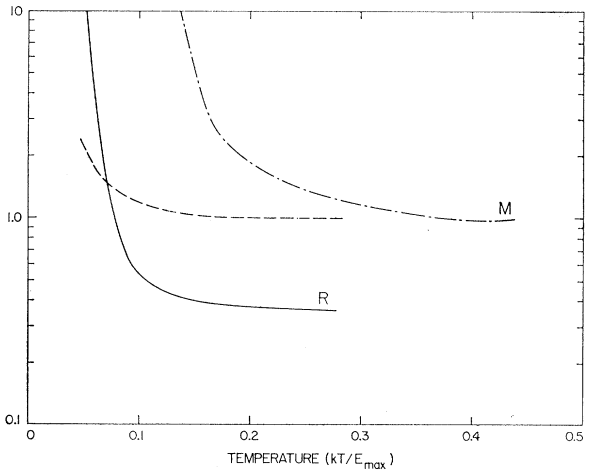

FIG. 5. Solid line is ratio of zero-field relaxation rates in MnF_2 and FeF_2. Dashed line is ratio of zero-field relaxation rate in FeF_2 and rate calculated assuming an Einstein spin-wave spectrum. This ratio is normalized to one at the highest temperature. M is the ratio of normalized magnetization deviation in MnF_2 and FeF_2. The temperature is in units of the maximum spin-wave energy.

[13] M. Butler, thesis, University of California at Santa Barbara, 1969 (unpublished).

where $\Delta m/m$ is the normalized magnetization deviation,[14] is also shown in Fig. 5. Both R and M rise sharply at low temperatures, indicating the larger energy gap in FeF_2. However, the knee in R occurs much lower ($0.1kT/E_{zB}$) than the knee in M at $\sim 0.2kT/E_{zB}$. This reflects the fact that T_1 is a two-magnon process and thus depends on the density of states squared, which tends to enhance the importance of the peak in the density of states, whereas Δm depends on a first-order process. This domination by the zone-boundary magnons is further evidenced by the reasonable agreement obtained when calculating the functional form of the relaxation rate using an Einstein-model spin-wave spectrum, i.e., a dispersionless spectrum (see Fig. 5).

CONCLUSIONS

The NSLR in FeF^{19}_2 has been measured in the temperature region 8–28°K. The results are in excellent agreement with the calculated relaxation rates for a two-magnon Raman scattering process. The calculation was based on a simplified dispersion relation which reduces the problem to a one-dimensional integral. This model adequately describes the total magnon density of states of generally cubic crystals in which the exchange interaction may be described by a single parameter. Utilizing this model, calculations of quantities such as T_1, which involve two-magnon scattering processes, are possible only when the spin-wave spectrum is relatively dispersionless. This is due to the sensitivity of the magnon scattering angle to anisotropy in the distribution of states in k space.

Comparison of these results with the MnF^{19}_2 results indicates that at relatively high temperatures NSLR is insensitive to changes in anisotropy, since second-order processes are dominated by the zone-boundary magnons.

ACKNOWLEDGMENT

We would like to thank Professor V. Jaccarino for reading the manuscript and for constructive criticisms.

APPENDIX: DERIVATION OF EQUATIONS (7a) AND (7b)

With the assumption of isotropic magnon dispersion, the dispersion relation becomes

$$E(q)=E_0[(1+\xi)^2-\cos^2(\tfrac{1}{2}q)]^{1/2}, \qquad \text{(A1)}$$

where $E_0=2z_2|J_2|S$. The Brillouin zone is spherical and of a radius π in q space; thus normalization requires

$$\frac{3}{4\pi^4}\int_0^{2\pi}\int_{-1}^{+1}\int_0^{\pi} q^2dqd\mu d\theta=1=\int_{E_{\min}}^{E_{\max}} D(E)dE. \qquad \text{(A2)}$$

[14] For comparison of FeF_2 and MnF_2 magnetizations see Ref. 10.

Since the energy only depends on the magnitude of q, the density of states may be written

$$D(E)=\frac{3}{\pi^3}q^2\left(\frac{dE}{dq}\right)^{-1}. \tag{A3}$$

Using Eq. (A1), we find

$$\frac{dE}{dq}=\frac{E_0^2}{2E}\cos\tfrac{1}{2}q\sin\tfrac{1}{2}q$$

and

$$\cos\tfrac{1}{2}q=[(1+\xi)^2-(E/E_0)^2]^{1/2}.$$

Using the identity

$$\sin^2x+\cos^2x=1$$

to show

$$\sin\tfrac{1}{2}q=[1+(E/E_0)^2-(1+\xi)^2]^{1/2},$$

and the identity

$$\sin x=2\sin\tfrac{1}{2}x\cos\tfrac{1}{2}x,$$

we obtain

$$q^2=\{\arcsin[2((1+\xi)^2-(E/E_0)^2)^{1/2}\times(1+(E/E_0)^2-(1+\xi)^2)^{1/2}]\}^2.$$

Thus the density of states for the isotropic magnon dispersion model is

$$D(E)=\frac{6E}{\pi^3E_0^2}\frac{\{\arcsin[2((1+\xi)^2-(E/E_0)^2)^{1/2}(1+(E/E_0)^2-(1+\xi)^2)^{1/2}]\}^2}{[(1+\xi)^2-(E/E_0)^2]^{1/2}[1+(E/E_0)^2-(1+\xi)^2]^{1/2}}. \tag{A4}$$

The Bose factor is defined

$$F(E)=e^{E/kT}/(e^{E/kT}-1)^2.$$

Equation (4b) may be written as a sum of four terms:

$$1/T_1'=(\pi/\hbar)(A+B-C-D), \tag{A5}$$

where

$$A=\frac{1}{N^2}\sum_{\mathbf{kk'}}[2(A_{zz}^{I})^2+(A_{zz}^{II})^2]\times(u_{\mathbf{k}}^2u_{\mathbf{k'}}^2+v_{\mathbf{k}}^2v_{\mathbf{k'}}^2)F(E)\delta(E_{\mathbf{k}}-E_{\mathbf{k'}}),$$

$$B=\frac{1}{N^2}\sum_{\mathbf{kk'}}2(A_{zz}^{I})^2(u_{\mathbf{k}}^2u_{\mathbf{k'}}^2+v_{\mathbf{k}}^2v_{\mathbf{k'}}^2)F(E)\times\cos[(\mathbf{k}-\mathbf{k'})\cdot(\mathbf{r}_I-\mathbf{r}_{I'})]\delta(E_{\mathbf{k}}-E_{\mathbf{k'}}),$$

$$C=\frac{1}{N^2}\sum_{\mathbf{kk'}}4A_{zz}^{I}A_{zz}^{II}u_{\mathbf{k}}u_{\mathbf{k'}}v_{\mathbf{k}}v_{\mathbf{k'}}F(E)\times\cos[(\mathbf{k}-\mathbf{k'})\cdot(\mathbf{r}_I-\mathbf{r}_{II})]\delta(E_{\mathbf{k}}-E_{\mathbf{k'}}),$$

and

$$D=\frac{1}{N^2}\sum_{\mathbf{kk'}}4A_{zz}^{I}A_{zz}^{II}u_{\mathbf{k}}u_{\mathbf{k'}}v_{\mathbf{k}}v_{\mathbf{k'}}F(E)\times\cos[(\mathbf{k}-\mathbf{k'})\cdot(\mathbf{r}_{I'}-\mathbf{r}_{II})]\delta(E_{\mathbf{k}}-E_{\mathbf{k'}}).$$

The u's and the v's are coefficients of a transformation which decouples the two sublattices. They are defined as[10]

$$u_k=\cosh\tfrac{1}{2}\theta_k,\quad v_k=-\sinh\tfrac{1}{2}\theta_k,$$

where

$$\tanh\theta_k=-(\cos\tfrac{1}{2}q)/(1+\xi)$$

and

$$u_k^2-v_k^2=1.$$

Writing these coefficients as a function of energy yields

$$u=\frac{E_0}{E}(1+\xi)\quad\text{and}\quad v=\frac{-E_0}{E}\left[(1+\xi)^2-\left(\frac{E}{E_0}\right)^2\right]^{1/2}.$$

Considering the terms in order and changing from sums over k space to integrals over energy by the following method:

$$\frac{1}{N}\sum_{\mathbf{k}}\rightarrow\int_{E_{\min}}^{E_{\max}}D(E)dE, \tag{A6}$$

we have

$$A=[2(A_{zz}^{I})^2+(A_{zz}^{II})^2]\sum_k\int F(E)D(E')\times[u^2(E)u^2(E')+v^2(E)v^2(E')]\delta(E-E')dE'.$$

Performing the integral is equivalent to replacing E' by E. Changing the second sum to an integral leads to the required expression for A:

$$A=[2(A_{zz}^{I})^2+(A_{zz}^{II})^2]\int_{E_{\min}}^{E_{\max}}D^2(E)F(E)\frac{E_0}{E}C(E)dE, \tag{A7}$$

where

$$C(E)=\left(\frac{E_0}{E}\right)^3\left\{(1+\xi)^4+\left[(1+\xi)^2-\left(\frac{E}{E_0}\right)^2\right]^2\right\}.$$

Term B may be written

$$B=\frac{12}{\pi^3}(A_{zz}^{I})^2\frac{1}{N}\sum_k\int_{-1}^{+1}\int_0^{\pi}F(E)(u_q^2u_{q'}^2+v_q^2v_{q'}^2)(q')^2\times\cos(q\mu-q'\mu')\frac{E}{E_0^2}\frac{\delta(q-q')}{\sin q}d\mu'dq',$$

where the energy δ function has been replaced by one in reduced space. Performing first the integration over q', we obtain

$$B=\frac{12}{\pi^3}(A_{zz}^{I})^2\frac{1}{N}\sum_k F(E)(u_k^4+v_k^4)q^2\times\frac{E}{E_0^2\sin q}\int_{-1}^{+1}\cos[q(\mu-\mu')]d\mu'.$$

As

$$\int_{-1}^{+1}\cos(a+bx)dx=\frac{2}{b}\cos a\sin b,$$

we find

$$B=\frac{24}{\pi^3}(A_{zz}{}^I)^2\frac{1}{N}\sum_k F(E)(u_k{}^4+v_k{}^4)q\frac{E}{E_0{}^2}\cos q\mu.$$

Replacing the second sum by an integral over q space,

$$B=\frac{36}{\pi^6}(A_{zz}{}^I)^2\int_0^\pi F(E)(u_k{}^4+v_k{}^4)q^3\frac{E}{E_0{}^2}\int_{-1}^{+1}\cos q\mu\,d\mu\,dq,$$

and then performing the integration over μ, we have

$$B=\frac{72}{\pi^6}(A_{zz}{}^I)^2\int_0^\pi F(E)(u_k{}^4+v_k{}^4)q^2\frac{E}{E_0{}^2}\sin q\,dq.$$

Converting the integral over the q space, one over energy finally yields

$$B=\frac{48}{\pi^3}(A_{zz}{}^I)^2\int_{E_{\min}}^{E_{\max}}F(E)D(E)\frac{E}{E_0{}^2}E_0{}^4/E^4\times\left\{(1+\xi)^4+\left[(1+\xi)^2-\left(\frac{E}{E_0}\right)^2\right]^2\right\}\times\left[(1+\xi)^2-\left(\frac{E}{E_0}\right)^2\right]^{1/2}\left[1+\left(\frac{E}{E_0}\right)^2-(1+\xi)^2\right]^{1/2}dE. \quad \text{(A8)}$$

By considering the magnetic unit cell for the rutile structure, it is possible to write $\mathbf{r}^I\mathbf{r}^{I\prime}$ and $\mathbf{r}^{II}$ in terms of the unit-cell dimensions. Then by going to q space and performing the appropriate rotation of the coordinates, it becomes obvious that C and D are equivalent and equal to

$$C=D=4A_{zz}{}^IA_{zz}{}^{II}\frac{1}{N^2}\sum_{\mathbf{q}\mathbf{q}'}u_{\mathbf{q}}u_{\mathbf{q}'}v_{\mathbf{q}}v_{\mathbf{q}'}F(E)\times\cos[\tfrac{1}{2}(q_z-q_z')]\delta(E_q-E_{q'}).$$

Converting the sum to an integral and the δ function to one in q space, we obtain

$$C=D=\frac{24A_{zz}{}^IA_{zz}{}^{II}}{N\pi^3}\sum_q\int_0^\pi\frac{E}{E_0{}^2}F(E)\times u_{\mathbf{q}}u_{\mathbf{q}'}v_{\mathbf{q}}v_{\mathbf{q}'}\delta(q-q')\frac{(q')^2}{\sin q'}\times\int_{-1}^{+1}\cos[\tfrac{1}{2}(q'\mu-q'\mu')]d\mu'dq'.$$

Carrying out these two integrations yields

$$C=D=\frac{96A_{zz}{}^IA_{zz}{}^{II}}{\pi^3}\frac{1}{N}\sum_q\frac{E}{E_0{}^2}F(E)u_q{}^2v_q{}^2\frac{q}{\sin q}\times\cos(\tfrac{1}{2}q\mu)\sin(\tfrac{1}{2}q).$$

Changing the second sum to an integral, we obtain

$$C=D=\frac{144A_{zz}{}^IA_{zz}{}^{II}}{\pi^6}\int_0^\pi\frac{E}{E_0{}^2}F(E)v_q{}^2u_q{}^2\times\frac{q^3\sin\frac{1}{2}q}{\sin q}\int_{-1}^{+1}\cos(\tfrac{1}{2}q\mu)d\mu dq.$$

Performing the angular integration and then converting to an integral over energy, we have

$$C=D=\frac{96A_{zz}{}^IA_{zz}{}^{II}}{\pi^3}\int_{E_{\min}}^{E_{\max}}F(E)D(E)\frac{E_0{}^2}{E^3}\times\left[(1+\xi)^2-\left(\frac{E}{E_0}\right)^2\right]^{1/2}\left[1+\left(\frac{E}{E_0}\right)^2-(1+\xi)^2\right]dE.$$

By using the identity

$$\sin^2(\tfrac{1}{2}x)=\tfrac{1}{2}(1-\cos x),$$

the zero-field two-magnon relaxation rate may be written as a sum of two terms:

$$1/T_1{}^0=(4\pi/\hbar)(A'-B'),$$

where

$$A'=\frac{1}{N^2}(A_{yz}{}^I)^2\sum_{\mathbf{k}\mathbf{k}'}\tfrac{1}{2}F(E)(u_{\mathbf{k}}{}^2u_{\mathbf{k}'}{}^2+v_{\mathbf{k}}{}^2v_{\mathbf{k}'}{}^2)\delta(E_{\mathbf{k}}-E_{\mathbf{k}'})$$

and

$$B'=\frac{1}{N^2}(A_{yz}{}^I)^2\sum_{\mathbf{k}\mathbf{k}'}\tfrac{1}{2}F(E)(u_{\mathbf{k}}{}^2u_{\mathbf{k}'}{}^2+v_{\mathbf{k}}{}^2v_{\mathbf{k}'}{}^2)\times\cos[(\mathbf{k}-\mathbf{k}')\cdot(\mathbf{r}^I-\mathbf{r}^{I\prime})]\times\delta(E_{\mathbf{k}}-E_{\mathbf{k}'}).$$

Noticing that

$$A'=A(A_{yz}{}^I)^2/2[2(A_{zz}{}^I)^2+(A_{zz}{}^{II})^2]$$

and

$$B'=B(A_{yz}{}^I)^2/4(A_{zz}{}^I)^2,$$

we have the necessary expressions to perform relaxation calculations for an isotropic magnon dispersion model. The energy integrals were calculated using an IBM 360 model 65.